ISSN No:-2456-2165 https://doi.org/10.38124/ijisrt/26nov1059

Autonomous Agricultural Rover

Anvesh[1]; Bheemashankar[2]; Bheemesha[3]; Jamadar Bhuvan[4]; Meenakshi Patil[5]

[1]Department of Electronics and Communication Engineering PDA College of Engineering Kalaburagi, India
[2]Department of Electronics and Communication Engineering PDA College of Engineering Kalaburagi, India
[3]Department of Electronics and Communication Engineering PDA College of Engineering Kalaburagi, India
[4]Department of Electronics and Communication Engineering PDA College of Engineering Kalaburagi, India
[5]Professor; Department of Electronics and Communication Engineering PDA College of Engineering Kalaburagi, India

Publication Date: 2026/11/25

Abstract: Leaf diseases weaken plants, and uniform manual spraying wastes agrochemicals and exposes farmers to harmful chemicals. This paper presents a low cost autonomous agricultural rover that locates plants, inspects their leaves, estimates disease severity, and sprays a matching dose. A Raspberry Pi 3B+ with a five megapixel camera on a two servo pan and tilt unit searches for plants by sweeping the pan axis. The rover then aligns with the plant, approaches it, and stops at fifteen centimeters using an ultrasonic sensor. The tilt servo adjusts the camera so that the leaf is in view, and a lightweight image classifier labels the leaf as healthy, low, medium, or high severity. A four channel relay module switches one of three pumps for three to four seconds according to the severity, after which the rover resumes its planned path. Two isolated battery packs keep motor noise away from the processor and prevent resets. Test results show a classification accuracy of 92 percent and a spraying success rate of 90 percent. The work shows that severity based spraying is practical on inexpensive embedded hardware.

Keywords: *Precision Agriculture, Raspberry Pi, Leaf Disease Detection, MobileNetV2, Autonomous Rover, Targeted Spraying.*

How to Cite: Anvesh; Bheemashankar; Bheemesha; Jamadar Bhuvan; Meenakshi Patil (2026) Autonomous Agricultural Rover. *International Journal of Innovative Science and Research Technology*, 11(11), 1460-1465. https://doi.org/10.38124/ijisrt/26nov1059

I. INTRODUCTION

Agricultural productivity relies heavily on timely crop protection against fungal, bacterial, and viral foliar pathogens. In conventional farming practices, agrochemicals—including fungicides, bactericides, and foliar nutrients—are applied uniformly across entire fields using manual knapsack sprayers or tractor-mounted boom sprayers. This blanket spraying paradigm treats healthy foliage identically to severely infected plants, resulting in up to 40–60% chemical wastage, elevated input costs for smallholder farmers, soil and groundwater contamination, and direct dermal or inhalation exposure of agricultural workers to toxic compounds.

Precision agriculture addresses these limitations by tailoring input delivery to the spatial and physiological needs of individual plants. Advances in embedded edge computing and quantized convolutional neural networks (CNNs) now enable real-time visual inspection directly on low-power single-board computers without requiring continuous cloud connectivity in rural fields. However, most existing agricultural prototypes either limit functionality to binary disease detection (healthy versus diseased) or trigger a single fixed-volume spray regardless of infection progression.

To bridge this gap, this paper presents the design, hardware integration, and field validation of a low-cost Autonomous Agricultural Rover capable of autonomous plant localization, two-axis leaf inspection, four-stage disease severity classification, and variable-dose targeted spraying. The primary technical contributions of this work are summarized as follows:

- Autonomous Edge-AI Rover Architecture: A self-contained mobile platform built around a Raspberry Pi 3B+ that executes plant detection, approach navigation, leaf alignment, and severity inference locally using an INT8-quantized MobileNetV2 model.
- Two-Axis Pan-and-Tilt Leaf Inspection: A dual-servo camera gimbal that sweeps horizontally to locate crop rows and adjusts vertically at a fixed 15 cm standoff distance to center leaves of varying canopy heights.
- Three-Tier Variable-Dose Spraying System: A four-channel opto-isolated relay module controlling three dedicated micro-pumps (low, medium, and high flow/concentration tiers) to match chemical dosage to estimated leaf severity while skipping healthy plants.
- Noise-Isolated Dual-Battery Power Design: Complete electrical isolation between the 12 V Li-ion logic supply and the 12 V lead-acid motor/pump rail, eliminating

ISSN No:-2456-2165 https://doi.org/10.38124/ijisrt/26nov1059

inductive voltage sags and processor brownout resets during actuation.

II. RELATED WORK

➢ *Existing Agricultural Spraying Robots*

Automated crop scouting and targeted spraying have attracted significant research interest over the past decade. Yilmaz et al. [1] developed an unmanned ground vehicle (UGV) for potato cultivation utilizing a YOLO object detector running on a Raspberry Pi 4B coupled with an adaptive neuro-fuzzy inference system (ANFIS) controller for navigation and spot disinfestation. While effective in open-row potato fields, the system relied on higher-cost compute hardware and binary target triggering.

Kachare et al. [2] proposed an image-processing-based fertilizer and pesticide spraying robot using a Raspberry Pi and servo-actuated nozzle positioning. Their work demonstrated the feasibility of color- and texture-based leaf segmentation on embedded Linux boards, though spraying duration remained uniform across detected targets. Similarly, Destreza et al. [3] introduced Smart Agribot, an automated spraying vehicle for green bean crops employing an EfficientDet CNN architecture to identify foliar lesions and activate a single solenoid spray valve.

➢ *Lightweight Deep Learning for Plant Pathology*

Deploying deep neural networks on resource-constrained microcomputers requires compact architectures with low multiply-accumulate (MAC) footprints. Sandler et al. [4] introduced MobileNetV2, which leverages inverted residual blocks and linear bottlenecks with depthwise separable convolutions to drastically reduce parameter count and inference latency. Subsequent studies in plant pathology, such as Mohanty et al. [5] and Hughes and Salathé [6], established large-scale leaf image benchmarks (PlantVillage) and validated transfer learning for multi-class foliar disease recognition. Furthermore, post-training integer quantization (FP32 to INT8) via TensorFlow Lite has been shown to accelerate ARM Cortex-A53 CPU inference by 2.5× to 3.5× with less than 1.5% accuracy degradation [7].

➢ *Research Gap and Motivation*

A comparative synthesis of existing literature reveals three recurring limitations: (1) reliance on computationally expensive GPUs or high-end single-board computers that increase bill-of-materials (BoM) cost beyond the reach of small farms; (2) fixed camera mounting angles that fail to capture leaves positioned at varying canopy elevations; and (3) binary spray actuation that delivers an identical chemical volume to early-stage and advanced infections. Our proposed system resolves these issues on an economical Raspberry Pi 3B+ by combining a pan-and-tilt active vision unit with a four-class severity classifier driving three distinct spray dosage channels.

III. SYSTEM ARCHITECTURE AND HARDWARE DESIGN

➢ *Overall System Architecture*

The autonomous rover is organized into four functional subsystems: (1) sensing and active vision, (2) embedded processing and web telemetry, (3) differential-drive locomotion, and (4) variable-dose fluid actuation. Fig. 1 illustrates the complete system block diagram, highlighting signal paths between peripherals and the isolated dual-battery power architecture.

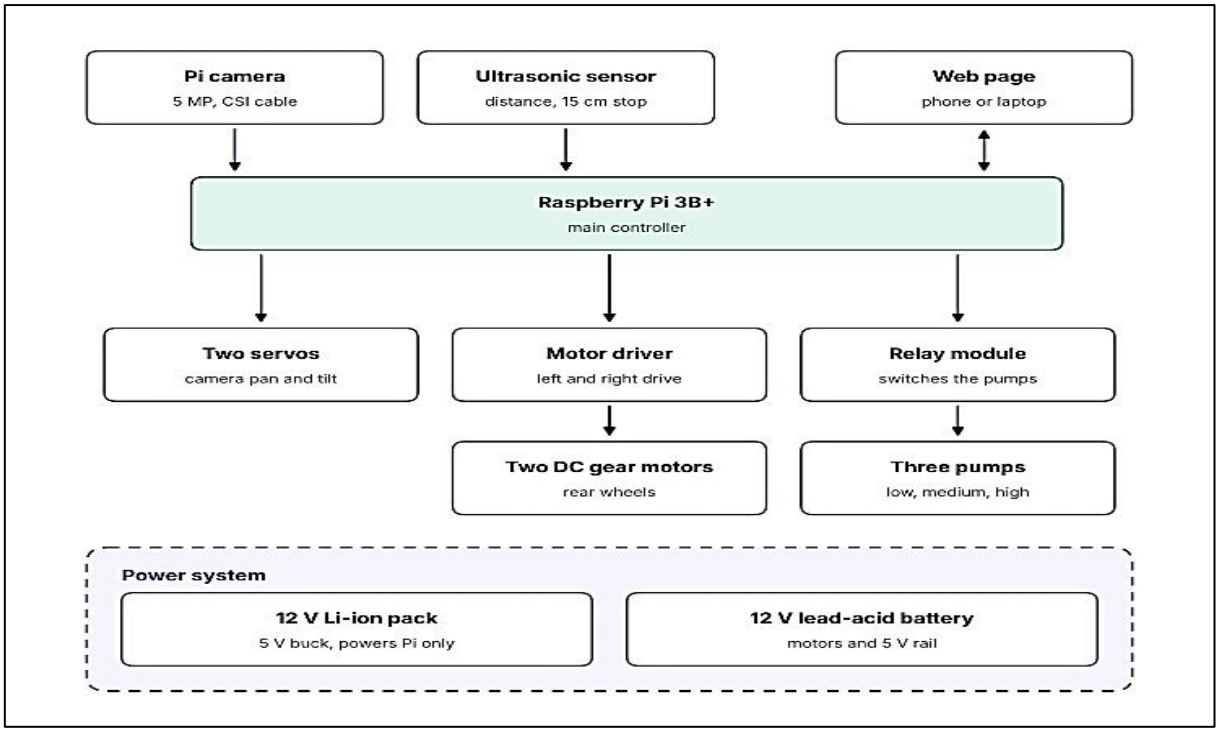


Fig 1 Overall System Block Diagram Showing the Raspberry Pi 3B+ Controller, Sensing/Actuation Interfaces, and Isolated Dual-Battery Power Architecture.

ISSN No:-2456-2165 https://doi.org/10.38124/ijisrt/26nov1059

A lightweight local web server hosted on the Raspberry Pi 3B+ provides a browser-based dashboard accessible over Wi-Fi from a smartphone or laptop. Operators can monitor live camera feeds, view classified disease severity scores, inspect ultrasonic standoff distance, and manually override drive or pump states during calibration.

➢ *Hardware Components and Pin-Level Interfacing*

The core processing unit is a Raspberry Pi 3 Model B+ featuring a 1.4 GHz 64-bit quad-core ARM Cortex-A53 processor and 1 GB LPDDR2 SDRAM. Table I summarizes the major hardware modules, electrical specifications, and functional roles within the rover.

Table 1 Hardware Components and Electrical Specifications

Subsystem / Component	Model / Rating	Interface & Role
Main Controller	Raspberry Pi 3B+ (1.4 GHz, 1 GB RAM)	Executes OpenCV search, TFLite inference, and state machine
Vision Sensor	5 MP OV5647 Pi Camera	15-pin MIPI CSI-2; captures 640×480 RGB frames
Pan-Tilt Gimbal	2× MG90S / SG90 Micro Servos	Hardware PWM (GPIO 12, 13); X-axis search & Y-axis leaf tilt
Range Sensor	HC-SR04 Ultrasonic (40 kHz)	GPIO Trigger/Echo via 1 kΩ/2 kΩ divider; stops rover at 15 cm
Motor Driver	L298N Dual H-Bridge (2 A/ch)	GPIO PWM + direction pins; drives rear differential wheels
Drive Motors	2× 12 V DC Geared Motors (100 RPM)	Rear-wheel differential drive with front caster/free wheels
Spray Switching	4-Channel 5 V Opto-Isolated Relay	Active-low GPIO control; switches 12 V pumps independently
Fluid Actuators	3× 12 V DC Diaphragm Mini-Pumps	Dedicated Low, Medium, and High dosage spray lines
Logic Battery	12 V Li-ion Pack + 5 V/3 A Buck	Dedicated isolated power rail for Raspberry Pi 3B+
Actuator Battery	12 V 7 Ah Sealed Lead-Acid	Supplies DC drive motors, spray pumps, and 5 V servo rail

To protect the 3.3 V non-tolerant GPIO pins of the Raspberry Pi 3B+ from the 5 V TTL ECHO pulse generated by the HC-SR04 ultrasonic sensor, a resistive voltage divider comprising R1 = 1 kΩ and R2 = 2 kΩ is connected between the ECHO pin and ground. The stepped-down voltage V_GPIO is given by:

$$V_{GPIO} = V_{ECHO} \times (R2 / (R1 + R2)) = 5.0\ V \times (2\ k\Omega / 3\ k\Omega) = 3.33\ V \quad (1)$$

This ensures reliable logic-high detection while preventing over-voltage stress on the BCM2837B0 SoC input buffer. Similarly, the 4-channel relay board incorporates PC817 optocouplers and freewheeling flyback diodes across each pump terminal to suppress inductive back-EMF spikes during pump turn-off.

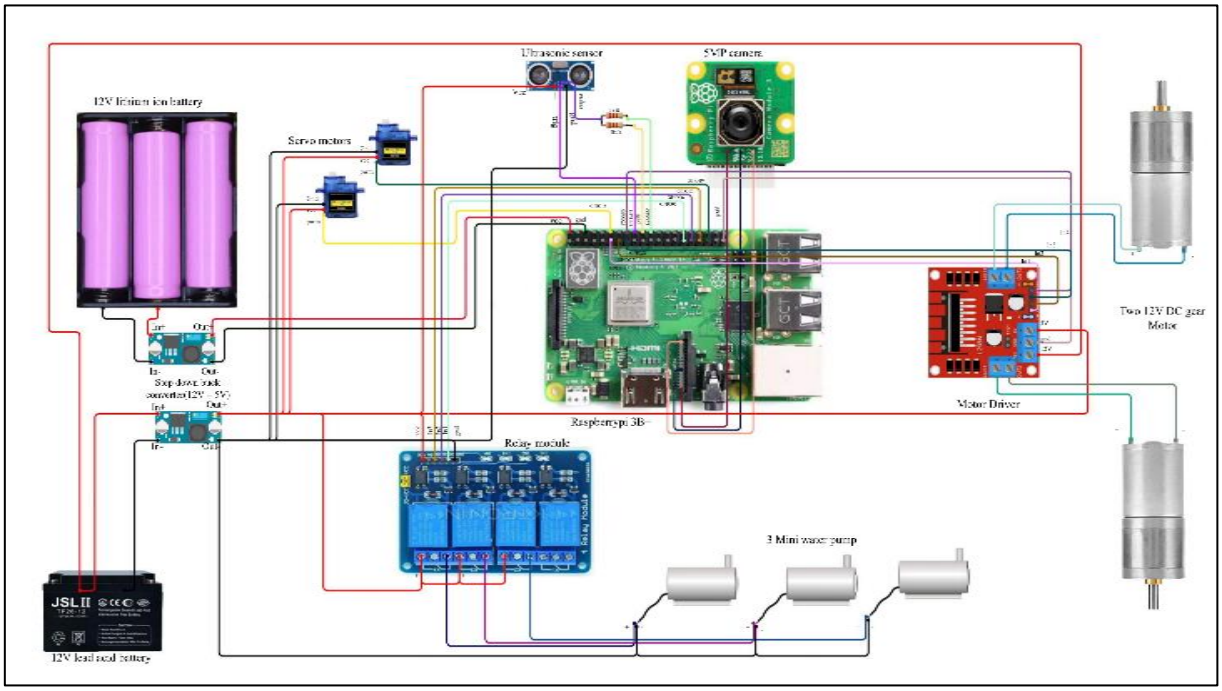


Fig 2 Complete Electronic Circuit Diagram

ISSN No:-2456-2165 https://doi.org/10.38124/ijisrt/26nov1059

➢ *Mechanical Chassis and Dual-Battery Isolation*

The mechanical frame is fabricated from rigid lightweight aluminum/acrylic extrusion rails providing high ground clearance for traversing uneven agricultural soil beds without damaging low-hanging foliage. Two 12 V high-torque DC gear motors coupled to wide-tread rubber wheels provide rear-wheel differential propulsion, while two front free-rotating caster wheels ensure zero-radius pivot turning during plant alignment. Three separate fluid reservoirs feed the three micro-pumps, terminating in an adjustable brass atomizing spray nozzle aligned coaxially with the camera field of view.

A critical engineering challenge in mobile agricultural robots is under-voltage brownout of the single-board computer when high-inrush DC motors or diaphragm pumps start simultaneously. In our design, the 12 V Lithium-ion battery pack exclusively powers the Raspberry Pi 3B+ via a high-efficiency LM2596 5 V/3 A buck converter, whereas a separate 12 V lead-acid battery supplies the L298N motor driver, three spray pumps, and an auxiliary 5 V regulator for the pan-tilt servos. Because the two power domains share only a low-impedance signal ground reference through opto-isolated/buffered interfaces, motor stall currents never induce voltage drops on the processor core rail.

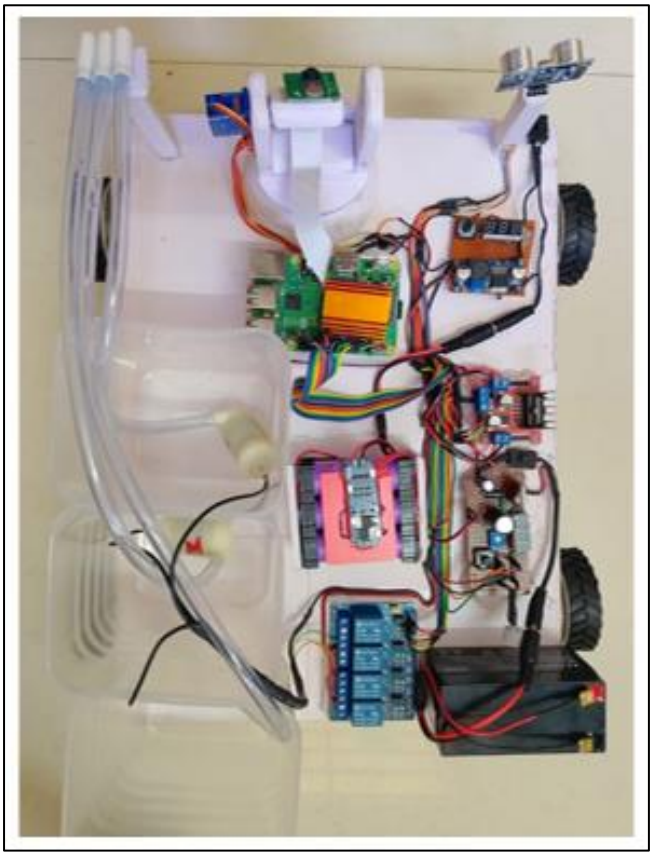




Fig 3 Assembled Hardware Prototype of the Autonomous Rover

➢ *Five-State Autonomous Navigation State Machine*

Rover operation is governed by a deterministic five-state finite state machine (FSM) implemented in Python using OpenCV, RPi.GPIO, and the TensorFlow Lite runtime. The behavioral transitions across field traversal are defined as follows:

- State 1 — Plant Search (Pan Sweep): While the chassis remains stationary, the horizontal pan servo sweeps across a 120° arc (-60° to +60°) in 5° increments. Captured frames are converted to the HSV color space and thresholded ($H \in [35, 85]$, $S \in [40, 255]$, $V \in [40, 255]$) to isolate green plant canopy regions from soil background.
- State 2 — Visual Servo Alignment and Approach: Once a green contour exceeding a minimum area threshold A_{min} is detected, the horizontal pixel error e_x between the contour centroid x_c and the image center x_0 drives differential wheel steering until $|e_x| < 20$ pixels. The rover then advances forward while polling the HC-SR04 sensor until the target standoff distance $d = 15$ cm is reached.
- State 3 — Vertical Leaf Centering (Tilt Scan): At the 15 cm inspection point, the vertical tilt servo adjusts the camera pitch angle θ_{tilt} in 3° steps until the target leaf region is centered vertically within the region of interest (ROI), ensuring consistent scale and framing across different plant heights.
- State 4 — Severity Inference and Variable Spraying: The centered leaf ROI is cropped, resized to 224×224 pixels, and passed to the quantized MobileNetV2 classifier. If classified as Healthy, spraying is bypassed. For Low, Medium, or High severity, the Raspberry Pi energizes relay channel 1, 2, or 3 for $t_{spray} \in [3.0\text{ s}, 4.0\text{ s}]$, delivering a calibrated chemical dose.
- State 5 — Gimbal Reset and Path Resumption: Upon completion of the spray cycle, both pan and tilt servos return to their neutral 0° home positions, a brief cooldown timer prevents re-triggering on the same plant, and the rover resumes forward row traversal.

ISSN No:-2456-2165 https://doi.org/10.38124/ijisrt/26nov1059

The ultrasonic standoff distance d (in centimeters) is computed from the round-trip echo pulse duration t (in seconds) using the speed of sound in air at ambient field temperature ($v \approx 34{,}300$ cm/s):

$$d = (t \times 34300) / 2 \quad (2)$$

To reject acoustic outliers caused by irregular leaf surfaces, a 5-sample median filter is applied to consecutive ultrasonic readings before issuing the motor brake command at $d \leq 15.0$ cm.

➢ *Disease Severity Dataset and MobileNetV2 Quantization*

To train a classifier capable of quantifying infection progression rather than merely detecting disease presence, leaf images were collected under natural outdoor illumination and annotated into four severity tiers based on the percentage of necrotic or chlorotic leaf area (PLA):

- Class 0 — Healthy (PLA = 0%): Uniformly green lamina without visible spots, lesions, or curling; triggers zero spray.
- Class 1 — Low Severity (0% < PLA ≤ 15%): Early-stage localized foliar spots; triggers Pump 1 (low-concentration prophylactic dose).
- Class 2 — Medium Severity (15% < PLA ≤ 40%): Moderate lesion coalescence across multiple leaf zones; triggers Pump 2 (standard therapeutic dose).
- Class 3 — High Severity (PLA > 40%): Extensive blight, necrosis, or leaf yellowing; triggers Pump 3 (high-potency curative dose).

Data augmentation—including random horizontal/vertical flips, ±25° rotations, brightness jitter (±20%), and random zoom—was applied during training to improve robustness against field lighting variations. A MobileNetV2 backbone pretrained on ImageNet was fine-tuned with a global average pooling layer, a 0.3 dropout layer, and a 4-unit softmax classification head using categorical cross-entropy loss and the Adam optimizer (learning rate 1×10^{-4}). After convergence, the floating-point (FP32) Keras model was converted into an 8-bit integer (INT8) quantized TensorFlow Lite (.tflite) flatbuffer using a representative calibration dataset, reducing model size from 9.2 MB to 2.6 MB and enabling sub-1.2 s CPU inference on the Raspberry Pi 3B+.

IV. EXPERIMENTAL RESULTS AND DISCUSSION

➢ *A Leaf Disease Severity Classification Performance*

The quantized INT8 MobileNetV2 model was evaluated on a held-out test set of field leaf images across all four severity categories. Classification performance was quantified using class-wise Precision, Recall, and F1-Score, defined as:

$$\text{Precision} = TP / (TP + FP), \quad \text{Recall} = TP / (TP + FN) \quad (3)$$

As detailed in Table 2, the model achieved an overall classification accuracy of 92.0% across the four classes. Healthy leaves exhibited the highest separability (0.96 precision, 0.97 recall), while High-severity leaves achieved 0.93 precision and 0.92 recall. Minor confusion occurred primarily between adjacent Low and Medium severity samples (F1-scores of 0.885 and 0.905, respectively), where lesion area percentages lay near the 15% boundary threshold.

Table 2 Class-Wise Disease Severity Classification Metrics

Severity Class	Affected Area	Precision	Recall	F1-Score
Healthy	0%	0.96	0.97	0.965
Low Severity	1% – 15%	0.89	0.88	0.885
Medium Severity	16% – 40%	0.90	0.91	0.905
High Severity	> 40%	0.93	0.92	0.925
Overall / Macro Avg.	All Classes	0.92	0.92	0.920

➢ *Stopping Accuracy, Spraying Reliability, and Runtime*

End-to-end physical trials were conducted to benchmark ultrasonic positioning accuracy, relay-pump actuation reliability, edge inference latency, and battery endurance. Across 10 repeated approach trials toward potted test plants with a target stopping distance of 15.0 cm, the rover achieved a mean absolute stopping error of 1.2 cm (stopping within 13.8 cm to 16.2 cm), well within the optimal atomization cone of the spray nozzle.

In targeted actuation tests, the rover selected and energized the exact pump corresponding to the ground-truth severity class in 90% of trials, maintaining a consistent 3.0 s to 4.0 s spray pulse duration. Table 3 summarizes the integrated field performance benchmarks.

Table 3 Integrated Rover System Performance Benchmarks

Evaluation Parameter	Measured Result	Operational Impact
Classification Accuracy	92.0%	Reliable 4-tier severity grading on edge CPU
Mean Stopping Distance Error	1.2 cm (at 15 cm target)	Maintains uniform nozzle-to-leaf spray cone
Correct Pump Selection Rate	90.0%	Accurate variable-dose chemical delivery
Spray Pulse Duration	3.0 s – 4.0 s	Controlled volume without leaf runoff
TFLite Inference Time	1.1 s / frame	Acceptable during stationary leaf inspection
Logic Battery Runtime	2.0 h – 3.0 h	Zero brownout resets under full pump load

ISSN No:-2456-2165 https://doi.org/10.38124/ijisrt/26nov1059

➢ *Comparative Analysis with Prior Systems*

Table 4 contrasts the proposed rover with recent agricultural spraying platforms reported in the literature, highlighting advantages in compute affordability, multi-axis leaf framing, and variable-dosage actuation.

Table 4 Comparison with Existing Agricultural Robots

Reference	Controller & Model	Camera Mount	Spraying Mode
Yilmaz et al. [1]	RPi 4B + YOLO-ANFIS	Fixed	Binary spot spray
Kachare et al. [2]	RPi + Classical CV	Servo nozzle	Uniform single dose
Destreza et al. [3]	Embedded + EfficientDet	Fixed	Single-valve spray
Proposed Rover	RPi 3B+ + INT8 MobileNetV2	2-Axis Pan & Tilt	3-Tier Severity Dose

➢ *Limitations and Practical Considerations*

While experimental trials validate the core architecture, three practical limitations were observed during outdoor testing: (1) Illumination Sensitivity: Because initial plant search relies on HSV color thresholding, harsh midday glare or deep canopy shadows can occasionally fragment green contours; (2) Dataset Generalization: Training images were acquired from a single local crop environment, requiring fine-tuning before deployment across visually distinct plant species; and (3) Open-Loop Odometry: Without wheel encoders or RTK-GPS feedback, long-distance inter-row navigation on sloped terrain is subject to gradual heading drift.

V. CONCLUSION AND FUTURE SCOPE

This paper presented a cost-effective Autonomous Agricultural Rover built on a Raspberry Pi 3B+ that integrates two-axis pan-and-tilt plant inspection, ultrasonic standoff control, INT8 MobileNetV2 disease severity grading, and three-channel variable-dose spraying. Experimental evaluation confirmed 92.0% severity classification accuracy, 1.1 s per-frame inference latency, 1.2 cm stopping precision at a 15 cm standoff, and 90.0% pump selection reliability, all protected from electrical resets by an isolated dual-battery power architecture. By skipping healthy foliage and scaling chemical application to infection severity, the system offers a practical pathway toward reducing agrochemical expenditure and environmental runoff in smallholder agriculture.

Future enhancements will focus on four upgrades: (1) replacing HSV color search with an ultra-lightweight single-stage detector (such as YOLOv8n or MobileNet-SSD) to eliminate sensitivity to ambient sunlight fluctuations; (2) integrating quadrature wheel encoders and an inertial measurement unit (IMU) for closed-loop row following; (3) expanding the training dataset across multiple regional crops and disease stages; and (4) adding solar trickle-charging and cloud-synced field disease heatmaps via the onboard web telemetry interface.

ACKNOWLEDGMENT

The authors express their sincere gratitude to Prof. Meenakshi Patil, Department of Electronics and Communication Engineering, PDA College of Engineering, Kalaburagi, for her valuable guidance and support throughout this project. The authors also thank Dr. Nagendra H, Head of the Department of Electronics and Communication Engineering, and the Principal of PDA College of Engineering, Kalaburagi, for providing the laboratory facilities and encouragement needed to complete this work.

REFERENCES

[1]. S. Yilmaz, D. Polat, E. B. Akboynuz, E. A. Gedikli, and Z. Yilmaz, “Detection and disinfestation of diseased plants with YOLO based ANFIS controlled unmanned ground vehicle,” in Proc. 3rd Cognitive Models and Artificial Intelligence Conf. (AICCONF), Prague, Czech Republic, 2025.

[2]. O. Kachare, V. Kale, B. N. Mohapatra, and N. Nehe, “Image processing based plant fertilizer spraying robot,” J. Process Manage. New Technol., vol. 13, no. 3-4, pp. 44–53, 2025.

[3]. F. G. Destreza, R. Concepcion Jr., J. A. Alano, J. J. De Padua, and K. J. Butiong, “Smart Agribot: Advanced CNN-based disease detection in green beans with EfficientDet and auto-spraying,” Int. J. Integr. Eng., vol. 17, no. 2, pp. 290–300, 2025.

[4]. M. Sandler, A. Howard, M. Zhu, A. Zhmoginov, and L.-C. Chen, “MobileNetV2: Inverted residuals and linear bottlenecks,” in Proc. IEEE/CVF Conf. Computer Vision and Pattern Recognition (CVPR), 2018, pp. 4510–4520.

[5]. S. P. Mohanty, D. P. Hughes, and M. Salathé, “Using deep learning for image-based plant disease detection,” Frontiers in Plant Science, vol. 7, Art. no. 1419, Sep. 2016.

[6]. D. P. Hughes and M. Salathé, “An open access repository of images on plant health to enable the development of mobile disease diagnostics,” arXiv preprint arXiv:1511.08060, 2015.

[7]. B. Jacob et al., “Quantization and training of neural networks for efficient integer-arithmetic-only inference,” in Proc. IEEE/CVF Conf. Computer Vision and Pattern Recognition (CVPR), 2018, pp. 2704–2713.

[8]. R. R. Shamshiri et al., “Research and development in agricultural robotics: A perspective of digital farming,” Int. J. Agric. Biol. Eng., vol. 11, no. 4, pp. 1–14, Jul. 2018.